Regular Article

PHYSICAL CHEMISTRY RESEARCH
Published by the
Iranian Chemical Society
www.physchemres.org
info@physchemres.org

Phys. Chem. Res., Vol. 12, No. 3, 821-835, September 2024
DOI: 10.22036/pcr.2024.422780.2440

Estimation of the Binding Affinities of Glycogen Phosphorylase Inhibitors by Molecular Docking to Support the Treatment of Type 2 Diabetes

T.Y. Vu[a], T.-T.-H. Le[b,c], T. Linh Pham[a], N.H. Hoang Vo[a], T.N. My Pham[a], M. Quan Pham[b,c,*] and H.T. Thu Phung[d,*]

[a]*Faculty of Pharmacy, Ton Duc Thang University, Ho Chi Minh City, Vietnam*
[b]*Institute of Natural Products Chemistry, Vietnam Academy of Science and Technology, Hanoi, Vietnam*
[c]*Graduate University of Science and Technology, Vietnam Academy of Science and Technology, Hanoi, Vietnam*
[d]*NTT Hi-Tech Institute, Nguyen Tat Thanh University, Ho Chi Minh City, Vietnam*
(Received 29 October 2023, Accepted 29 January 2024)

In the current landscape of drug discovery, various docking programs for virtual database screening significantly reduce costs and time. This study re-docked twenty-three known inhibitors of glycogen phosphorylase (GP), a key target for type 2 diabetes (T2D) therapy, using seven methods including Autodock 4 (AD4), AutoDockVina (Vina), modified Vina (mVina), Standard Precision mode (SP) and Extra Precision mode (XP) of Glide methods, Molecular Operating Environment (MOE) and Genetic Optimization for Ligand Docking (GOLD). Results showed that GOLD showed the worst computational precision with the highest RMSE of 20.98 kcal mol^{-1}. Conversely, MOE was the most precise with the lowest RMSE of 1.99 kcal mol^{-1}, closely followed by AD4 (2.27 kcal mol^{-1}). However, MOE failed to generate the correct ligand-binding pose, showing a 0% success rate in docking for all RMSD resolutions (<0.2, 0.15, and 0.1 nm). Among the top-performing methods, GOLD surpassed others in docking success rates for GP ligands, achieving 96% success at RMSD < 0.2 nm, compared to 74%, 70%, and 74% for AD4, Vina, and mVina, respectively. These four packages can produce a ligand-binding posture that closely resembles the crystal structure discovered through experimental studies. The findings serve as the foundation for selecting an appropriate tool for screening candidate drugs for the T2D therapeutic target.

Keywords: Docking programs, Glycogen phosphorylase, Autodock, Glide docking, MOE, GOLD

INTRODUCTION

Recent advancements in computational chemistry have significantly impacted drug discovery methodologies [1,2]. These techniques, such as Density Functional Theory (DFT) and molecular docking, explored across a variety of compounds, have proven effective in elucidating molecular interactions and properties of potential therapeutics, offering critical insights into their structural and electronic aspects [3-5]. This efficiency enhances the drug development process, facilitating the rapid and cost-effective identification of new therapeutic agents. Furthermore, molecular docking, recognized for evaluating ligand binding affinity to target proteins [6-9], has gained prominence due to its versatility and precision. Demonstrated by various studies [10-13], it effectively forms stable complexes with enzymes and receptors, providing valuable insights into compounds' potential as enzyme inhibitors or anticancer agents. The field has seen the development of a myriad of docking servers, software packages, and applications, each employing unique force fields and algorithms. Free open-source docking tools that may quickly ascertain the ligand binding affinity can be mentioned as Autodock4 (AD4) [14], Autodock Vina (Vina)

*Corresponding authors. E-mail: ptthuong@ntt.edu.vn; pham-minh.quan@inpc.vast.vn

[15], mVina (an experimental parameter correction version of Vina) [16], and molecular operating environment (MOE) [17]. Besides, well-established commercial packages such as Glide standard precision (SP) and extra precision (XP) [18-20] and Genetic Optimization for Ligand Docking (GOLD) [21] have also been widely used as scoring functions for the protein-ligand docking program.

Worldwide, about 10% of the population has been affected by diabetes mellitus, a chronic condition, which is characterized by the body's inability to effectively regulate blood sugar levels [22,23]. There are two main types: Type 1, where the body fails to produce sufficient insulin [24], and Type 2, characterized by the body's resistance to insulin or insufficient production [25]. Managing diabetes typically involves lifestyle changes, monitoring blood glucose levels, and medication [26]. For Type 1 diabetes, insulin therapy remains the cornerstone, with advancements in insulin types and delivery methods improving patient experiences [27]. More than 90% of diabetic patients have type 2 diabetes (T2D), which is frequently linked to obesity [23]. The incidence and prevalence of T2D are rising internationally despite a better understanding of the risk factors for the illness and evidence of effective preventative programs. Numerous researchers have looked at the etiology of T2D in an effort to create better treatments [25]. T2D thus sees a broader array of drugs [28], including metformin, which enhances the body's response to insulin [29], and various other classes like sulfonylureas [30], DPP-4 inhibitors [31], and GLP-1 receptor agonists [32], each with unique mechanisms to manage blood sugar levels. Furthermore, recent developments in SGLT2 inhibitors offer not only blood sugar control but also cardiovascular and kidney benefits [33,34].

Glycogen phosphorylase (GP), which catalyzes the first stage of glycogen phosphorolysis in the liver, has emerged as a potential target in T2D treatment. GP catalyzes the phosphorolytic cleavage of glycogen at the α-1,4-glycosidic bond, producing glucose 1-phosphate (G-1-P) and a glycogen polymer that is one sugar residue shorter [35]. Different GP inhibitors have been discovered and can be divided into 2 groups, the first is the inhibitors suppressing GP by directly binding to the enzyme via the active site, azasugar site, AMP site, indole-binding site, purine-nucleoside site, and glycogen-storage site, and the second is the inhibitors that can indirectly suppress gluconeogenesis by interfering with glucose/glycogen cycling [35].

While molecular and pharmacological data shows that inhibiting GP is an appealing method for lowering hyperglycemia in T2Ds, there are a number of problems and concerns about safety and effectiveness. The most crucial unanswered question is whether or not persistent GP inhibition may lower blood glucose levels in T2Ds by a level that is clinically relevant. The GP inhibitors that have been identified so far do not show a lot of selectivity for the GP isoform in the liver [35] due to the high homology of GP isoenzymes between skeletal muscle and liver and the conserved binding site for GP inhibitors throughout isoenzymes [36]. In light of the ongoing quest for effective GP inhibitors, this study represents a significant advancement by conducting a comprehensive comparison of seven docking software packages, including AD4, Vina, mVina, SP, XP, MOE, and GOLD. This marks the first time such a broad range of software tools has been evaluated side-by-side specifically for GP inhibitors. Our objective is to meticulously evaluate each software's efficacy in different metrics, such as precision in computation, pose accuracy, and successful docking rates. This holistic assessment aims to guide future researchers in selecting the most appropriate and efficient software for screening potential GP inhibitors, serving as the foundation for the discovery of new drugs for T2D treatment.

MATERIALS AND METHODS

Parameterized Complexes

The initial structures of twenty-three GP-ligand complexes were obtained from the Protein Data Bank (PDB), including 1AXR [37], 1GGN [38], 1HLF [38], 1K06 [39], 1K08 [39], 1KTI [39], 1NOJ [40], 1NOK [40], 2G9Q [41], 2PRJ [42], 2QRG [43], 2QRH [43], 2QRM [43], 2QRP [43], 2QRQ [43], 3G2H [44], 3G2I [44], 3G2J [44], 3G2K [44], 3G2L [44], 3G2N [44], 3SYM [45] and 3SYR [45]. The generation of parameters for rigid proteins and flexible ligands was accomplished using AutodockTools 1.5.6 [14]. These parameters were then recorded as files in the PDBQT format (Protein Data Bank with Partial Charge – Q and Atom Type – T). In order to represent both the receptor and ligand, a unified atom model with polar hydrogen atoms was

employed [46]. To predict atomic charges for the proteins, the Gasteiger-Marsili method was utilized [47,48].

Molecular Docking *via* AutoDock Vina and mVina

Re-docking, also known as the method of re-binding the ligand to the corresponding target receptor, aims to evaluate whether the algorithm and prediction parameters are consistent with the experimental ones. The re-docking model is shown in Fig. 1.

The Vina scoring function is entirely empirical and includes terms for hydrophobic and torsion forces as well as hydrogen bonds, repulsion, and Gaussian steric interactions [15]. While mVina has the experimental parameters altered to improve the ability to rank ligand binding affinities [16]. Molecular docking was conducted using both the Vina package and mVina (https://github.com/sontungngo/mvina.git). The global searching parameter was set to the *short* option of 8. For the Vina docking grid center, the center of mass of the ligand was selected from the experimental pose (x = 33.899 Å; y = 23.574 Å; z = 29.130 Å). The docking grid was identified to be 20 × 20 × 20 $Å^3$ in order to completely cover the target active site. The maximum energy difference between the worst and best docking profiles was set at 7 kcal mol^{-1}. The lowest binding free energy mode was then determined from the docking conformations.

Molecular Docking *via* AD4

The semiempirical AD4 scoring function includes a Coulomb potential term, a Lennard-Jones 12-6 potential term, a desolvation term linked to volume, and a conformational entropy term related to the quantity of rotational bonds [14]. Using the same grid center as Vina docking, AutoDock 4.2 docking simulations were performed. Autogrid4 was employed to generate a 60 × 60 × 60 Å grid with a grid spacing of 0.375 Å. A genetic algorithm (GA) run of 10 was selected, with a population size and generation number of 150 and 27,000, respectively. The GA number of evaluations was set at 250,000, equivalent to the short option. The conformational cluster with the lowest binding free energy was identified as the optimal docking model. Furthermore, the AutoDock 4.2 method produced 120,000 ligand poses. The ligand-binding affinity was determined as the average binding free energy of the entire conformation defined in the cluster.

Molecular Docking *via* Glide Standard Precision and Extra Precision

Glide approximates a full systematic search of the conformational, orientational, and positional space of the docked ligand, in contrast to existing approaches for docking ligands to the hard 3D structure of a known protein receptor [18]. Compared to the standard scoring function SP, XP introduces novel terms into the binding free energy scoring function, significantly improving Glide's ability to identify known active chemicals from a random ligand library [20]. Glide docking simulations were run using the SP [18, 19] and XP [20] scoring functions. Maestro's "Protein Preparation Wizard" and Ligprep were used to generate the receptors and ligands, respectively. The docking settings were set to

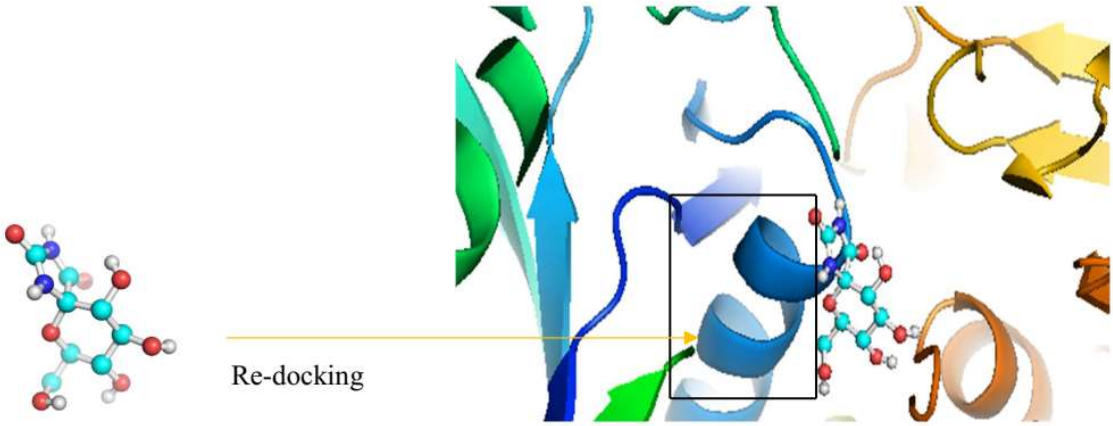

Fig. 1. Re-docking model of representative ligand to GP protein.

default, and 10 docking postures were generated during the simulations. The conformation with the highest ligand-binding affinity was selected.

Molecular Docking *via* MOE

MOE's docking package utilizes an intricate blend of scoring functions and sophisticated algorithms, intricately assessing the interaction dynamics between a ligand and its target protein [17]. Specifically for docking, MOE uses an algorithm known as the "Triangle Matcher" for pose generation, followed by a refinement process using the London dG scoring function. The MOE 2015.10 software was utilized to prepare the ligands and proteins for docking simulations. The MOE QuickPrep tools were used to convert the ligands into their respective 3D structures, which were then used as input files. The ligand energy was minimized using the MMFF94x force field until a gradient of 0.01 was achieved. Following energy minimization, the proteins were prepared for docking by protonation Protonate 3D tools implemented in MOE. Due to the limited resolution of most macromolecular crystal structures, these structures typically have little or no hydrogen coordinate data. The Amber99 force field was employed for energy minimization up to a 0.01 gradient following protonation. The Triangular Matching docking method was used to dock the ligands into the protein's active site, and 100 conformations of each ligand-protein complex were generated with docking scores.

Molecular Docking *via* GOLD

GOLD employs a sophisticated genetic algorithm to predict the binding poses of ligands in protein targets [21]. It generates multiple ligand conformations, assesses their fit within the protein binding site using a detailed scoring function, and optimizes these poses iteratively [21]. This process not only determines the most feasible binding configurations but also estimates the ligand's binding affinity, crucial for evaluating potential drug efficacy. GOLD v.5.7.3 software was used to dock the GP inhibitors. During each run, a population of 10 individuals underwent several GA operations. The operator weights for crossover, mutation, and migration were set to their standard default values of 95, 95, and 10, respectively. The cutoff value for van der Waals was 2.5 and the distance for hydrogen bonds (HB) was set to 3.5 Å.

Structural Analysis

Using GROMACS tools [49], the root-mean-square deviation (RMSD) was calculated between two structures. The interactions of the docked poses of ligand-GP complexes were then illustrated using either Pymol or BIOVIA Discovery Studio Visualizer software.

RESULTS

Estimated Ligand-Binding Free Energy

Table 1 displays the free binding energy calculations of 23 ligands with GP using seven software packages. To increase the likelihood of accuracy, only the results with the lowest free binding energy or best binding affinity are taken into account. The docking scores produced by six out of the seven software packages ranged from -15.5 to -4.75 kcal mol^{-1}, with the majority of free binding energies falling below -5.0 kcal mol^{-1}. However, GOLD produced values that were unrealistically negative. It's important to note that the seven docking methods employed did not factor in the complexity of the system's dynamics, the influence of the explicit solvent, or the ligand's restricted docking position. As a result, this could lead to a decrease in the accuracy of predicting protein-ligand binding affinity.

The smaller the root-mean-square error (RMSE), the higher the accuracy of the method. The RMSE values between the docking and experimental data when using the seven methods are shown in Table 2. The results show that MOE had the highest precision calculation and GOLD had the lowest. Among the five remaining techniques, AD4 produces the most accurate estimation of ligand-binding affinity, followed by Vina and SP, and XP and mVina. In addition, the standard error (SE) of the mean binding-free energy ΔG_{pre} obtained by MOE was the smallest, followed by AD4, Vina, and SP, respectively. Meanwhile, the SE value for GOLD was the highest, followed by those of XP and mVina (Table 2). Together, it is shown that the MOE docking method converged faster than the other approaches, while GOLD failed to calculate the proper binding free energy of GP ligands.

The initial ligand structure was related to the docking success rate, where the ligand conformation was considered the successful binding conformation when the RMSD of atomic positions from the corresponding experimental

Table 1. Free Binding Energy Predicted by Five Docking Software Packages. The Experimental Affinity ΔG_{exp} was Estimated *via* the Equation $\Delta G = -RT \ln k_i$, where k_i is the Inhibition Constant, R is the Gas Constant and T is the Absolute Temperature

No.	Complex	ΔG_{exp} (kcal mol^{-1})	ΔG_{pre} (kcal mol^{-1})						
			AD4	Vina	mVina	SP	XP	MOE	GOLD
1	1NOK	-4.33	-6.70	-7.50	-9.70	-8.78	-10.01	-6.56	-23.30
2	2PRJ	-6.17	-6.26	-7.80	-10.20	-8.57	-12.25	-7.27	-27.40
3	2G9Q	-8.78	-4.73	-5.40	-6.40	-7.11	-6.72	-5.52	-20.70
4	2QRP	-8.51	-10.30	-12.20	-17.00	-9.80	-13.10	-9.56	-34.72
5	3G2K	-6.58	-11.22	-11.70	-17.00	-10.82	-12.89	-8.80	-32.30
6	3SYR	-7.00	-8.17	-9.10	-12.70	-10.91	-12.92	-8.13	-56.66
7	3G2H	-5.24	-7.58	-9.60	-13.30	-4.75	-5.43	-7.87	-30.14
8	1KTI	-4.71	-7.09	-9.00	-12.10	-8.48	-11.15	-7.65	-22.46
9	3SYM	-6.27	-7.07	-9.50	-13.20	-11.41	-13.94	-7.84	-23.78
10	1NOJ	-4.33	-6.86	-7.40	-9.40	-7.62	-9.62	-6.26	-19.20
11	3G2I	-6.68	-6.60	-8.80	-12.10	-9.54	-12.88	-7.80	-22.14
12	3G2J	-6.52	-6.27	-8.10	-10.80	-8.93	-12.68	-7.36	-24.97
13	2QRQ	-7.00	-8.01	-10.10	-13.90	-9.80	-13.10	-7.84	-10.48
14	2QRH	-6.46	-8.80	-10.30	-14.00	-10.27	-13.17	-8.37	-32.52
15	2QRG	-7.11	-9.59	-10.50	-14.80	-10.84	-14.52	-8.42	-9.67
16	2QRM	-5.54	-8.65	-10.80	-15.50	-10.71	-12.55	-8.66	-4.08
17	1GGN	-7.56	-5.53	-8.60	-11.10	-9.57	-13.66	-6.62	-21.01
18	1AXR	-4.49	-6.88	-7.20	-9.70	-8.88	-11.43	-6.16	-23.65
19	1HLF	-7.74	-6.95	-8.10	-11.00	-9.44	-10.30	-6.66	-43.35
20	3G2N	-5.62	-7.35	-9.00	-12.60	-9.68	-12.89	-8.00	-29.09
21	3G2L	-5.31	-9.30	-10.00	-14.80	-10.05	-12.12	-8.92	-32.12
22	1K08	-7.33	-7.35	-9.70	-13.60	-6.75	-7.64	-8.86	-25.67
23	1K06	-7.33	-6.95	-9.60	-13.60	-9.44	-14.93	-8.63	-25.23

Table 2. RMSE and SE of Seven Docking Packages

	AD4	Vina	mVina	SP	XP	MOE	GOLD
RMSE (kcal mol^{-1})	2.27	3.29	6.71	3.41	5.99	1.99	20.98
SE (kcal mol^{-1})	0.32	0.32	0.53	0.33	0.52	0.22	2.27

structure was less than 0.2 nm [50]. The results of calculating the RMSD value are shown in Table 3 accordingly, and they reveal that GOLD possesses the smallest mean $RMSD_{GOLD}$ of 0.08 ± 0.01 nm, indicating that GOLD efficiently constructs the accurate binding pose for GP ligands. Interestingly, the three approaches, including AD4, Vina, and mVina, produced comparable accuracy in the determination of the ligand-binding pose. In particular, the mean values $RMSD_{AD4/Vina/mVia}$ between experimental structures and docked shapes using three protocols were 0.09 ± 0.02 nm. Meanwhile, the average RMSD of SP, XP, and MOE was significantly higher at 0.2 ± 0.46, 0.4 ± 0.11, and

Table 3. RMSD Values of the Seven Docking Methods

No.	Complex	RMSD (nm)						
		AD4	Vina	mVina	SP	XP	MOE	GOLD
1	1NOK	0.03	0.02	0.02	0.07	0.10	0.27	0.02
2	2PRJ	0.07	0.02	0.06	0.11	0.05	0.34	0.01
3	2G9Q	0.01	0.03	0.03	0.67	0.63	0.2	0.1
4	2QRP	0.04	0.05	0.05	0.09	1.61	0.57	0.07
5	3G2K	0.15	0.05	0.05	0.10	1.65	0.56	0.09
6	3SYR	0.05	0.05	0.05	0.06	0.06	0.39	0.02
7	3G2H	0.04	0.06	0.08	0.46	0.46	0.44	0.03
8	1KTI	0.04	0.06	0.06	0.07	0.08	0.4	0.17
9	3SYM	0.05	0.06	0.07	0.33	0.33	0.4	0.06
10	1NOJ	0.04	0.07	0.07	0.05	0.05	0.28	0.06
11	3G2I	0.10	0.08	0.08	0.11	0.11	0.42	0.08
12	3G2J	0.07	0.09	0.07	0.57	0.57	0.36	0.07
13	2QRQ	0.05	0.11	0.10	0.09	1.61	0.47	0.17
14	2QRH	0.10	0.11	0.11	0.07	0.07	0.45	0.02
15	2QRG	0.05	0.11	0.11	0.33	0.32	0.53	0.17
16	2QRM	0.12	0.12	0.12	0.66	0.66	0.53	0.2
17	1GGN	0.25	0.25	0.26	0.07	0.05	0.3	0.05
18	1AXR	0.28	0.28	0.27	0.08	0.08	0.31	0.06
19	1HLF	0.37	0.37	0.36	0.10	0.07	0.28	0.01
20	3G2N	0.10	0.40	0.05	0.06	0.06	0.43	0.04
21	3G2L	0.41	0.48	0.48	0.07	0.07	0.46	0.03
22	1K08	0.55	0.55	0.57	0.66	0.86	0.53	0.14
23	1K06	0.56	0.56	0.57	0.20	0.46	0.52	0.1

0.41 ± 0.02 nm, respectively, pointing out that these three methods did not generate proper ligand-binding poses. It should be noted that the computed error is the standard error of the mean.

It is clearly the case that the higher the docking success rate, the more suitable the method is for ligand-binding pose identification because the docking ratio represents the probability of finding the native binding pose compared to the experimental structure. Considering RMSD values smaller than 0.2, 0.15, and 0.1 nm, respectively, the percentage of docking success changes accordingly (Fig. 2). As expected, GOLD had the best docking success rate among all tested methods, showing up to 96% at RMSD < 0.2 nm, 83% at RMSD < 0.15 nm, and 70% at RMSD < 0.1 nm. The docking success rates of AD4, Vina, and mVina were 74%, 70%, and 74%, respectively, at RMSD values below 0.2 and 0.15 nm. At the RMSD value < 0.1 nm, the successful-docking percentage decreased by 65%, 52%, and 61%, respectively, for the three methods. Meanwhile, the docking success rates of SP were 70% and 61% at the resolution of RMSD below 0.2 and 0.15 nm, respectively. When the RMSD was less than 0.1 nm, the rate dropped quickly to 48%. Regarding XP, when RMSD was less than 0.2 and 0.15 nm, the successful-docking percentage was only 52%, and

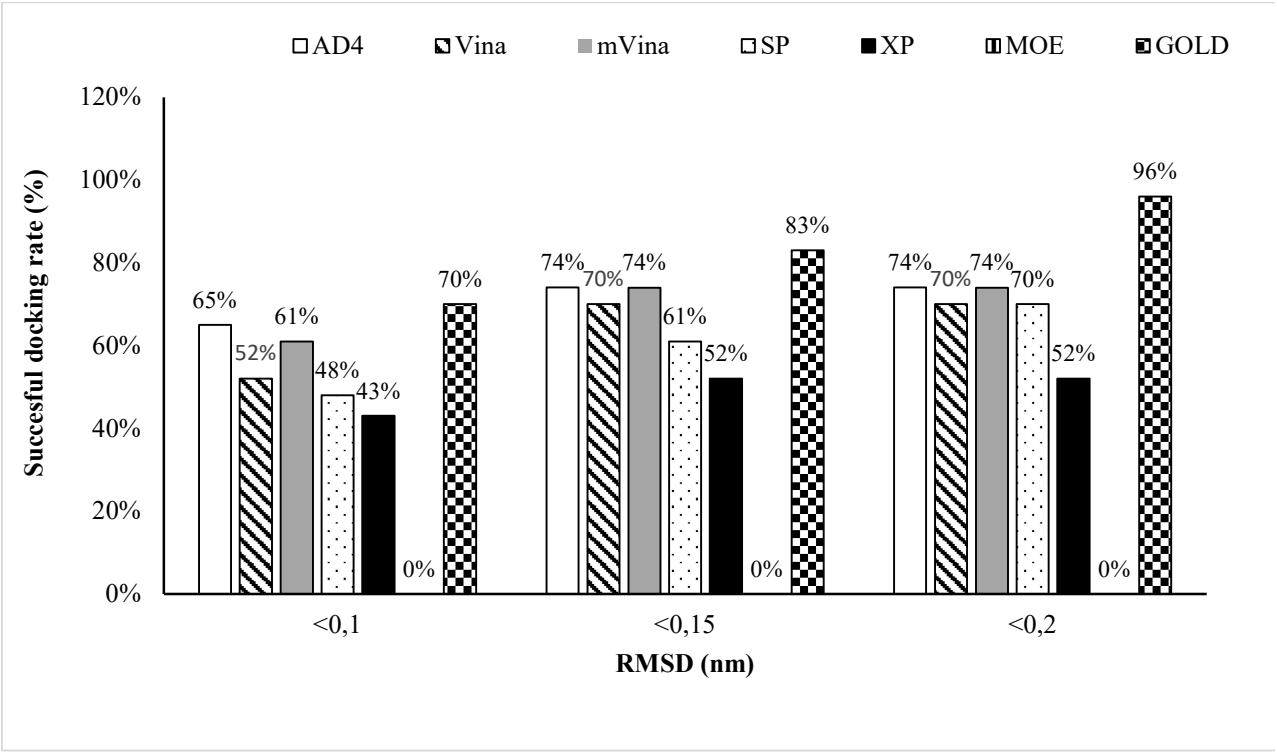

Fig. 2. Successful docking rates were obtained *via* seven protocols upon various resolutions.

the rate got as low as 43% at the resolution of RMSD < 0.1 nm. There is no doubt that MOE possessed an extremely poor docking success rate of as low as 0% regarding all resolutions of RMSD values, proving that this technique cannot generate the precise binding pose of GP ligands. Overall, except for XP, SP, and MOE, the four docking methods including AD4, Vina, mVina and GOLD always give a high success percentage (>50%), but GOLD has a superior docking success rate compared to the other three methods.

Redocked Binding Pose

All-atom molecular dynamic (MD) simulations were routinely used to validate docking results. The ligand-binding position appears to be a significant element since it is linked to the accuracy of free energy calculations using MD simulations. To study the ligand-receptor interaction, the input molecular structure is very important. If the docking position is far from the initial position, the MD simulation takes a long time to bring the system to equilibrium. If the system is poorly controlled, it may reach a false equilibrium. As a result, the accuracy of binding affinity estimation is greatly reduced. Therefore, it is required to conduct an assessment of docking position, rank docking poses compared to the experimental data, and obtain which software generates docking poses closest to the original. Hence, the subsequent MD simulation will be shorter and more accurate accordingly. Four docking packages including AD4, Vina, mVina, and GOLD were shown above to produce suitable docking binding poses for GP ligands. Here, the binding structures of representative GP inhibitors gained by AD4 and GOLD methods are subsequently analyzed.

Binding poses by AD4. The GP enzyme exists in two forms: a comparatively inactive form GP(*b*) and a more catalytically active form GP(*a*). Reversible phosphorylation, which changes the inactive *b* form (T state) into its active *a* form (R state), is the primary regulation mechanism in the liver [51]. Figure 3 shows the interaction between N-acetyl-beta-D-glucopyranosylamine (NBG) and the binding site of GP (*b* form) obtained via re-docking NBG into the complex ID 2PRJ [42] by AD4. The amino acids of GP involved in the interaction with NBG predicted by redocking were Asn284, Glu672, His377, Ser674, and Gly675. A HB is formed from

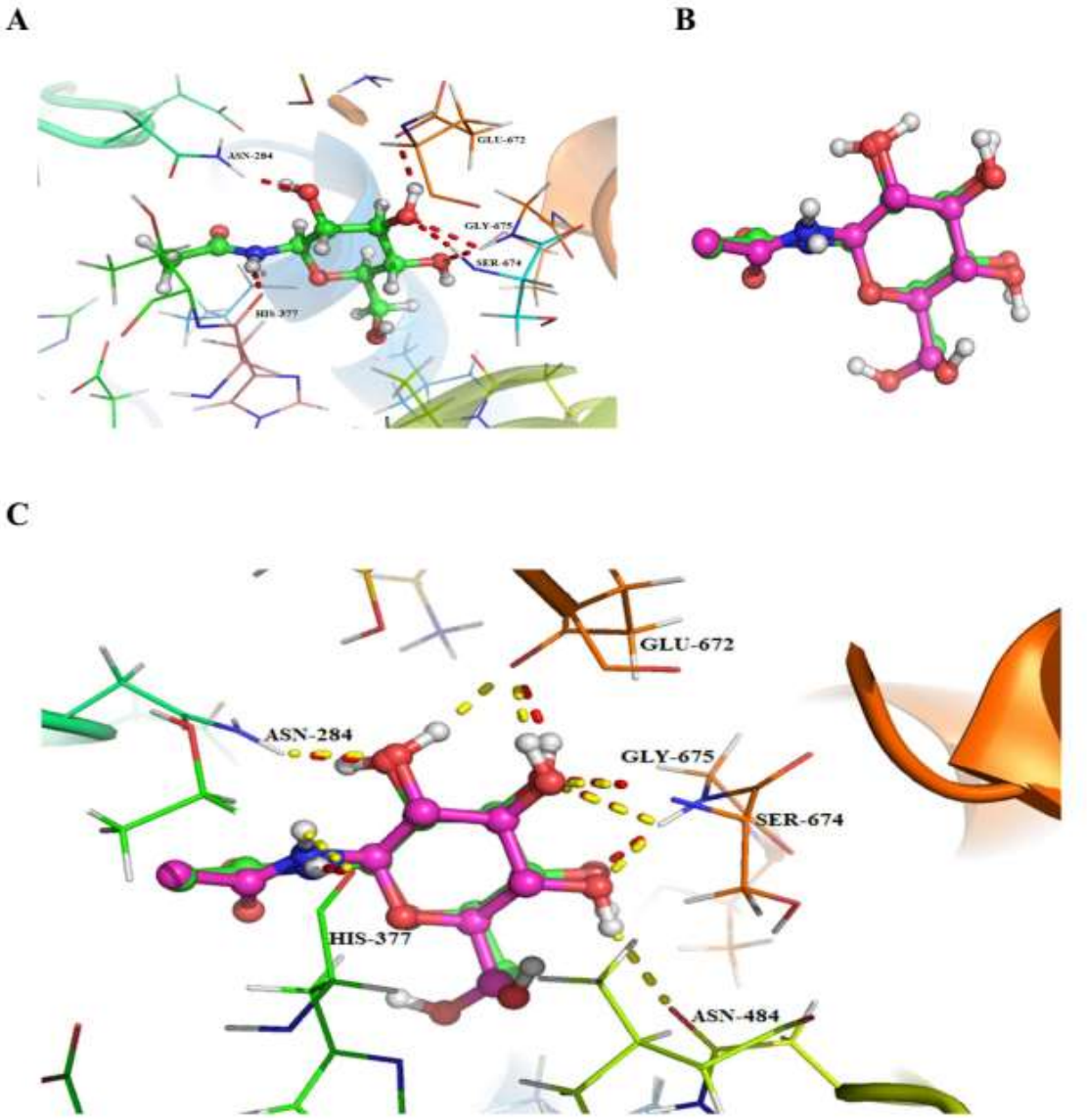

Fig. 3. Interaction of NBG ligand in the complex 2PRJ. (A) Detailed 3D interaction between the NBG ligand and GP protein was obtained *via* re-docking simulations using the AD4 package. The carbon atom of NBG is green, red represents the oxygen atom (O), blue is nitrogen (N) and hydrogen (H) is white. (B) Match of the ligand NBG in the complex 2PRJ attained *via* X-ray crystal structure and docking simulations. (C) Compatibility of ligand NBG from X-ray crystal structure (green C atom) and docking simulations (pink C atom). The red hyphen represents the GP-NBG interaction predicted *via* docking calculations, and the yellow hyphen represents the interaction obtained *via* experiment.

(-OH-C2) of NBG as the hydrogen acceptor, and (-NH) of Asn284 as a hydrogen donor, which stabilizes the 280s loop of GP [51]. The (-OH-C3) of NBG is the hydrogen donor and the (C=O) group of Glu672 is the hydrogen acceptor, forming the second HB. The third HB is made up of (-OH-C3) as the hydrogen acceptor and (-NH) of Ser674 as the hydrogen donor. Also, the same position (-OH-C3) is the hydrogen acceptor, and (-NH) of Gly675 is the hydrogen donor, creating an additional HB. A fifth HB is formed between (-OH-C4) as the hydrogen acceptor and (-NH) of Gly675 as

the hydrogen donor. A sixth HB is established between the (-NH) group of the ligand and the (C=O) group of His377, with the distance estimated to be approximately 2.9 Å (Fig. 3A). The docking simulation via AD4 software gave an RMSD value of 0.07 nm (Table 2), leading to a high match between the two positions of NBG in the docking and X-ray crystal structures (Figure 3B). As a consequence, the GP-NBG complex structure acquired from the X-ray crystallization and docking simulations has a high degree of similarity compared to each other (Fig. 3C). NBG makes a total of 12 HBs with GP identified by crystallization [42], agreeing with those of Asn284, Glu672, His377, Ser674 and Gly675 predicted by AD4.

(A) Detailed 3D interaction between the NBG ligand and GP protein was obtained via re-docking simulations using the AD4 package. The carbon atom of NBG is green, red represents the oxygen atom (O), blue is nitrogen (N) and hydrogen (H) is white. (B) Match of the ligand NBG in the complex 2PRJ attained via X-ray crystal structure and docking simulations. (C) Compatibility of ligand NBG from X-ray crystal structure (green C atom) and docking simulations (pink C atom). The red hyphen represents the GP-NBG interaction predicted via docking calculations, and the yellow hyphen represents the interaction obtained via experiment.

Binding poses by GOLD. The interacting conformation between (2S,5S,7R,9S)-8,9,10-trihydroxy-7-(hydroxymethyl)-2-mercapto-6-oxa-1,3-diazaspiro[4.5] decan-4-one (GL4) and the active site of GP*b* in the complex ID 1HLF [38] predicted by GOLD is shown in Fig. 4. Gly135, Leu136, Asn284, His377, Ser674, and Gly675 were identified as the GP amino acids interacting with GL4, resulting in a total of seven HBs. Two HBs are formed when the (C=O) group at C4 of GL4 acts as a hydrogen acceptor and the (-NH) groups of Gly135 and Leu136 in the main chain act as hydrogen donors. The (-NH-C1) group of GL4 is the hydrogen donor, and the (C=O) group of His377 is the hydrogen acceptor, resulting in the formation of the third HB. The fourth HB is made up of the hydrogen acceptor (-OH-CH2-C7) and the (-NH) of Gly135. Three HBs are formed between the hydrogen acceptors (-OH-C9) and (-OH-C10) positions of the GL4 ligand and the hydrogen donors (-NH) groups of Ser674 and Gly675, respectively. Because of the calculated RMSD value of 0.01 nm, it is obvious that GOLD can highly predict the precise binding pose between GL4 and GP (Table 2). Crystallographic studies revealed that GL4 forms thirteen HBs with GPb [38]. A comparison of the interaction of GL4 with GP obtained by GOLD and a crystallographic experiment reported a strong match in ligand position as well as the same GP interacting amino acids (Figs. 4B and C).

(A) Detailed 3D interaction between the GL4 ligand and GP protein was obtained via re-docking simulations using the GOLD package. The carbon atom of GL4 is green, red represents the oxygen atom (O), blue is nitrogen (N) and hydrogen (H) is white. (B) Match of the ligand GL4 in the complex 1HLF attained *via* X-ray crystal structure and GOLD docking simulations. (C) Compatibility of GL4 ligand from X-ray crystal structures (green C atom) and docking simulations (pink C atom). The red hyphen represents the GP-GL4 interaction predicted via docking calculations, and the yellow hyphen represents the interaction obtained via experiment.

DISCUSSIONS

The best docking program is a question that is frequently asked. Different studies have tried to compare the benefits and drawbacks of the software measured against various benchmarks, serving as general benchmarks when selecting a docking program for a specific application [52-54]. Using multiple docking programs is advised to result in a better assessment of protein-ligand interactions and more accurate pose ranking [55,56]. Scoring functions and search algorithms are the two key components of molecular docking packages, such as AD4, Vina, mVina, Glide, MOE, and GOLD. The scoring function is used to predict the binding affinity between a protein and a ligand, while the search algorithm is used to find the most favorable orientation of the ligand in the binding site. Scoring functions typically calculate the protein-ligand interaction energy and consider various energy terms such as van der Waals interactions, hydrogen bonding, and electrostatic interactions. AD4 uses a linear combination of energy terms to obtain the final score, while Vina uses a scoring function based on molecular mechanics and molecular dynamics simulations. Glide uses a combination of molecular mechanics, molecular dynamics, and free energy calculations to predict the binding affinity,

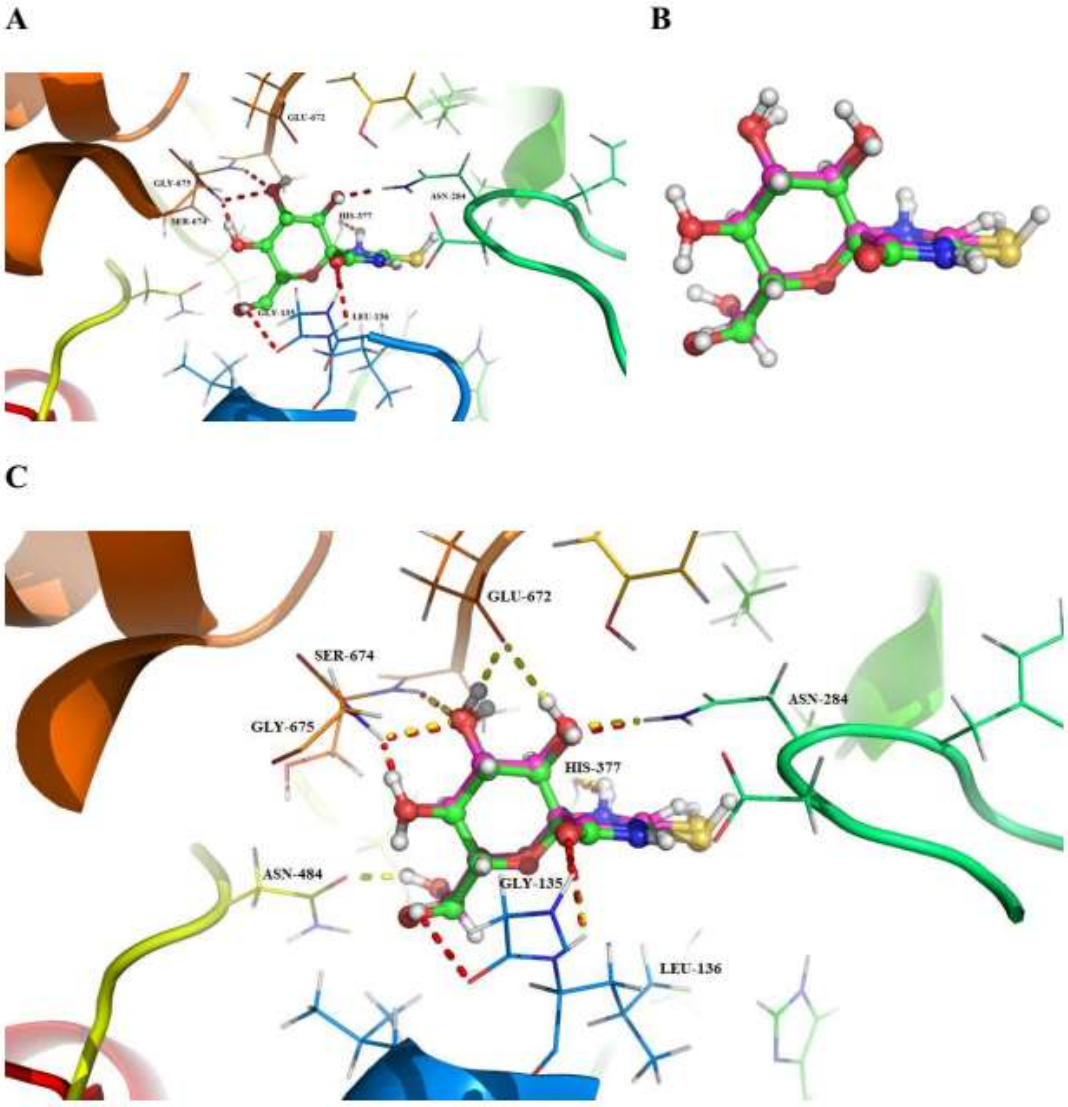

Fig. 4. Interaction of GL4 ligand in the complex 1HLF. (A) Detailed 3D interaction between the GL4 ligand and GP protein was obtained *via* re-docking simulations using the GOLD package. The carbon atom of GL4 is green, red represents the oxygen atom (O), blue is nitrogen (N) and hydrogen (H) is white. (B) Match of the ligand GL4 in the complex 1HLF attained *via* X-ray crystal structure and GOLD docking simulations. (C) Compatibility of GL4 ligand from X-ray crystal structures (green C atom) and docking simulations (pink C atom). The red hyphen represents the GP-GL4 interaction predicted *via* docking calculations, and the yellow hyphen represents the interaction obtained *via* experiment.

while MOE uses molecular mechanics calculations. Finally, GOLD uses free energy calculations and molecular mechanics simulations to predict the binding affinity. The search algorithms used in molecular docking packages range from simple heuristics to more sophisticated global optimization methods. AD4 uses a Lamarckian genetic algorithm (LGA) while Vina uses a combined global and local search algorithm. Glide uses a grid-based refinement method and a Monte Carlo optimization approach. MOE uses a modified version of the LGA called the Lamarckian-

Genetic Algorithm with Eigenvector Tracking (LGA-ET). GOLD uses a combination of a genetic algorithm, stochastic search, and dynamic programming to generate its predictions [57]. Each of these packages has its own strengths and weaknesses and is suited for different types of molecular docking applications.

Vina has been accessible since 2010, whereas AD4 was made public in 2009, and nowadays, both are frequently utilized because they are Windows-friendly approaches. Several strong inhibitors that bind to peptides, proteins, and genes were found thanks to the work of AD4 [58,59]. Vina is quite simple to use and has gained more acceptance than AD4 in recent years because Vina was found to be more reliable than AD4 in determining the ligand-binding affinity [60]. Due to its powerful computing capabilities, Vina has been used to predict the binding pose of big substrates to protein targets [61,62] as well as to estimate the binding affinities of small compounds to biomolecular targets such as peptides, proteins, and genes [63,64]. Nevertheless, Vina results in a high docking success rate but a low correlation coefficient between predicted and experimental binding affinity [65], hampering the ranking of the ligand-binding affinity. Therefore, mVina with experimental parameter correction was established to improve the ability to rank binding affinity [16].

MOE and GOLD tend to have a slight edge in terms of accuracy compared to Glide, but the difference can vary depending on the specific application. MOE and GOLD are known for their advanced features for handling flexible ligands and proteins, making them a good choice for applications where ligand flexibility is important. Glide's grid-based refinement method may not be as effective in handling flexible systems but is still capable of handling small to medium-sized systems. MOE, GOLD, and Glide are all user-friendly interfaces with visualization tools. Previously, MOE was believed to be one of the most user-friendly platforms with a wide range of tools beyond docking [57].

It is no doubt that docking calculations have helped to significantly cut down costs and time in new drug research. However, molecular docking has limitations, just like any other technique. Although there are many reliable docking programs available, it should be noted that not all docking algorithms are appropriate for every system [66]. Here, we carried out re-docking of 23 GP inhibitors identified using AD4, Vina, mVina, Glide XP and SP, MOE, and GOLD approaches. A comparison of the outputs indicates that, except for GOLD, six other software packages produce reasonable binding affinities for GP ligands. In particular, MOE possessed the highest precision calculation of the ligand-binding affinity. However, this package totally failed to produce the proper binding structure for GP ligands. Although all four docking techniques including AD4, Vina, mVina, and GOLD provide high docking success rates, GOLD outperforms the other three methods. Nevertheless, GOLD was unable to estimate the proper binding free energy of GP ligands. Additionally, the AD4, Vina, mVina, and GOLD packages can generate the ligand binding pose that well matches the crystal structure obtained by practical experiments. The input structure is close to the experimental structure, and the simulation time of MD is short, rapidly bringing the system to equilibrium.

The results obtained in this study will be the basis for choosing a suitable support tool in the screening of potential compounds for GP, the T2D treatment target. Natural compounds provide a wide range of structures for the discovery of novel and effective GP inhibitors. Functional foods and pharmaceuticals are also developing rapidly with computer assistance in the process of finding new drugs for T2Ds. Thanks to the structural flexibility of GP, the five docking techniques have been found to have advantageous effects in ligand library screening. Furthermore, the design of structure-based drugs that target allosteric sites such as GP is challenging, but using a docking method with a high success rate is an important basis for taking the next steps in the new drug discovery process.

CONCLUSION

This study marks a significant stride in the search for effective GP inhibitors by offering a detailed comparison of seven docking software tools: AD4, Vina, mVina, SP, XP, MOE, and GOLD. It's a pioneering effort to evaluate such a diverse array of software specifically for GP inhibitors. Key findings include MOE's high precision in binding energy calculations, with the lowest RMSE, counterbalanced by its failure to accurately predict ligand-binding poses. In contrast, GOLD, despite its worst precision in binding energy with the

highest RMSE, excelled in ligand-binding pose prediction with the best docking success rate. Other software packages like AD4, Vina, and mVina showed balanced performance in both precision and docking success rates, with moderate RMSE and success rates. SP and XP, however, did not exhibit notable performance in either metric.

The findings highlight the criticality of choosing the right software aligned with the specific goals of ligand library screening. MOE is ideal for projects where binding energy precision is vital, while GOLD is preferable for accurate ligand positioning. For a more balanced approach, AD4, Vina, or mVina are recommended. This study not only aids in the strategic tool selection for GP inhibitor screening but also paves the way for faster development of new T2D therapies.

ACKNOWLEDGMENT

The authors especially thank Dr. Son Tung Ngo at the Laboratory of Theoretical and Computational Biophysics, Ton Duc Thang University, Ho Chi Minh City, Vietnam for comments and valuable discussion.

REFERENCES

[1] Yu, W.; MacKerell, A. D., *Computer-aided drug design methods*, Antibiotics, Springer: **2017**, pp. 85-106.

[2] Marshall, G. R., Computer-aided drug design, *Annu. Rev. Pharmacol. Toxicol.*, **1987**, *27*, 193-213, DOI: 10.1146/annurev.pa.27.040187.001205.

[3] Kumar, A. R.; Ilavarasan, L.; Mol, G. S.; Selvaraj, S.; Azam, M.; Jayaprakash, P.; Kesavan, M.; Alam, M.; Dhanalakshmi, J.; Al-Resayes, S. I., Spectroscopic (FT-IR, FT-Raman, UV-Vis and NMR) and computational (DFT, MESP, NBO, NCI, LOL, ELF, RDG and QTAIM) profiling of 5-chloro-2-hydroxy-3-methoxybenzaldehyde: A promising antitumor agent, *J. Mol. Struct.*, **2024**, *1298*, 136974,

[4] Kanagathara, N.; Marchewka, M.; Thirunavukkarasu, M.; Selvaraj, S.; Janczak, J.; Lo, A. -Y., Structural and vibrational characterizations, DFT calculations, second harmonic generation, molecular docking studies on L-argininium 3, 3-dimethylacrylate, *Mater. Chem. Phys.*, **2023**, *307*, 128166.

[5] Rajkumar, P.; Selvaraj, S.; Anthoniammal, P.; Kumar, A. R.; Kasthuri, K.; Kumaresan, S., Structural (monomer and dimer), spectroscopic (FT-IR, FT-Raman, UV-Vis and NMR) and solvent effect (polar and nonpolar) studies of 2-methoxy-4-vinyl phenol, *Chemical Physics Impact*, **2023**, *7*, 100257,

[6] McDonnell, J. R.; Reynolds, R. G.; Fogel, D. B., *Docking conformationally flexible small molecules into a protein binding site through evolutionary programming*, Evolutionary Programming IV: Proceedings of the Fourth Annual Conference on Evolutionary Programming, The MIT Press: **1995**, pp. 615-627.

[7] Sousa, S. F.; Fernandes, P. A.; Ramos, M. J., Protein-ligand docking: current status and future challenges, *Proteins: Struct. Funct. Bioinform.*, **2006**, *65*, 15-26, DOI: 10.1002/prot.21082. PMID: 16862531.

[8] Irwin, J. J.; Shoichet, B. K., Docking screens for novel ligands conferring new biology, *J. Med. Chem.*, **2016**, *59*, 4103-4120, DOI: 10.1021/acs.jmedchem.5b02008.

[9] Zhang, B.; Li, H.; Yu, K.; Jin, Z., Molecular docking-based computational platform for high-throughput virtual screening, *CCF Trans. High Perform. Comput.*, **2022**, *4*, 63-74, DOI: 10.1007/s42514-021-00086-5.

[10] Kumar A, R. S., Sankar, In Silico Studies on the Molecular Geometry, FMO, Mulliken Charges, MESP, ADME and Molecular Docking Prediction of Pyrogallol Carboxaldehydes as Potential Anti-tumour Agents, *Physical Chemistry Research*, **2024**, *12*, 305-320,

[11] Ram Kumar, A.; Kanagathara, N., Spectroscopic, Structural and Molecular Docking Studies on N, N-Dimethyl-2-[6-methyl-2-(4-methylphenyl) Imidazo [1, 2-a] pyridin-3-yl] Acetamide, *Physical Chemistry Research*, **2024**, *12*, 95-107,

[12] Ram Kumar, A.; Selvaraj, S.; Azam, M.; Sheeja Mol, G.; Kanagathara, N.; Alam, M.; Jayaprakash, P., Spectroscopic, biological, and topological insights on lemonol as a potential anticancer agent, *ACS omega*, **2023**, *8*, 31548-31566,

[13] Kumar, A. R.; Selvaraj, S.; Anthoniammal, P.; Ramalingam, R. J.; Balu, R.; Jayaprakash, P.; Mol, G. S., Comparison of spectroscopic, structural, and molecular docking studies of 5-nitro-2-fluoroaniline and 2-nitro-5-fluoroaniline: An attempt on fluoroaniline isomers, *J. Fluorine Chem.*, **2023**, *270*, 110167.

[14] Morris, G. M.; Huey, R.; Lindstrom, W.; Sanner, M. F.;

Belew, R. K.; Goodsell, D. S.; Olson, A. J., AutoDock4 and AutoDockTools4: Automated docking with selective receptor flexibility, *J. Comput. Chem.*, **2009**, *30*, 2785-2791, DOI: org/10.1002/jcc.21256.

[15] Trott, O.; Olson, A. J., AutoDock Vina: improving the speed and accuracy of docking with a new scoring function, efficient optimization, and multithreading, *J. Comput. Chem.*, **2010**, *31*, 455-461, DOI: 10.1002/jcc.21334.

[16] Pham, T. N. H.; Nguyen, T. H.; Tam, N. M.; T, Y. V.; Pham, N. T.; Huy, N. T.; Mai, B. K.; Tung, N. T.; Pham, M. Q.; V, V. V.; Ngo, S. T., Improving ligand-ranking of AutoDock Vina by changing the empirical parameters, *J. Comput. Chem.*, **2022**, *43*, 160-169, DOI: 10.1002/jcc.26779.

[17] Vilar, S.; Cozza, G.; Moro, S., Medicinal chemistry and the molecular operating environment (MOE): application of QSAR and molecular docking to drug discovery, *Curr. Top. Med. Chem.*, **2008**, *8*, 1555-1572, DOI: org/10.2174/156802608786786624.

[18] Friesner, R. A.; Banks, J. L.; Murphy, R. B.; Halgren, T. A.; Klicic, J. J.; Mainz, D. T.; Repasky, M. P.; Knoll, E. H.; Shelley, M.; Perry, J. K.; Shaw, D. E.; Francis, P.; Shenkin, P. S., Glide: A New Approach for Rapid, Accurate Docking and Scoring. 1. Method and Assessment of Docking Accuracy, *J. Med. Chem.*, **2004**, *47*, 1739-1749, DOI: 10.1021/jm0306430.

[19] Halgren, T. A.; Murphy, R. B.; Friesner, R. A.; Beard, H. S.; Frye, L. L.; Pollard, W. T.; Banks, J. L., Glide: A New Approach for Rapid, Accurate Docking and Scoring. 2. Enrichment Factors in Database Screening, *J. Med. Chem*, **2004**, *47*, 1750-1759, DOI: 10.1021/jm030644s.

[20] Friesner, R. A.; Murphy, R. B.; Repasky, M. P.; Frye, L. L.; Greenwood, J. R.; Halgren, T. A.; Sanschagrin, P. C.; Mainz, D. T., Extra precision glide: Docking and scoring incorporating a model of hydrophobic enclosure for protein− ligand complexes, *J. Med. Chem.*, **2006**, *49*, 6177-6196, DOI: org/10.1021/jm051256o.

[21] Jones, G.; Willett, P.; Glen, R. C.; Leach, A. R.; Taylor, R., Development and validation of a genetic algorithm for flexible docking, *J. Mol. Biol.*, **1997**, *267*, 727-748, DOI: org/10.1006/jmbi.1996.0897.

[22] Zimmet, P. Z.; Magliano, D. J.; Herman, W. H.; Shaw, J. E., Diabetes: a 21st century challenge, *The Lancet Diabetes & endocrinology*, **2014**, *2*, 56-64.

[23]Taylor, S. I.; Yazdi, Z. S.; Beitelshees, A. L., Pharmacological treatment of hyperglycemia in type 2 diabetes, *J. Clin. Invest.*, **2021**, *131*, DOI: 10.1172/JCI142243.

[24] Atkinson, M. A.; Eisenbarth, G. S.; Michels, A. W., Type 1 diabetes, *The Lancet*, **2014**, *383*, 69-82.

[25] Chatterjee, S.; Khunti, K.; Davies, M. J., Type 2 diabetes, *The Lancet*, **2017**, *389*, 2239-2251, DOI: org/10.1016/S0140-6736(22)01655-5.

[26] Nathan, D. M., Diabetes: advances in diagnosis and treatment, *JAMA*, **2015**, *314*, 1052-1062.

[27] Atkinson, M. A.; Eisenbarth, G. S., Type 1 diabetes: new perspectives on disease pathogenesis and treatment, *The Lancet*, **2001**, *358*, 221-229,

[28] Nauck, M. A.; Wefers, J.; Meier, J. J., Treatment of type 2 diabetes: challenges, hopes, and anticipated successes, *The Lancet Diabetes & Endocrinology*, **2021**, *9*, 525-544.

[29] Rojas, L. B. A.; Gomes, M. B., Metformin: an old but still the best treatment for type 2 diabetes, *Diabetol. Metab. Syndr.*, **2013**, *5*, 1-15.

[30] Rendell, M., The role of sulphonylureas in the management of type 2 diabetes mellitus, *Drugs*, **2004**, *64*, 1339-1358.

[31] Scheen, A., DPP-4 inhibitors in the management of type 2 diabetes: a critical review of head-to-head trials, *Diabetes Metab.*, **2012**, *38*, 89-101.

[32] Nauck, M. A.; Quast, D. R.; Wefers, J.; Meier, J. J., GLP-1 receptor agonists in the treatment of type 2 diabetes-state-of-the-art, *Molecular metabolism*, **2021**, *46*, 101102.

[33] Nauck, M. A., Update on developments with SGLT2 inhibitors in the management of type 2 diabetes, *Drug design, development and therapy*, **2014**, 1380-1380.

[34] Saisho, Y., SGLT2 inhibitors: the star in the treatment of type 2 diabetes?, *Diseases*, **2020**, *8*, 14.

[35] Henke, B. R.; Sparks, S. M., Glycogen phosphorylase inhibitors, *Mini Rev. Med. Chem.*, **2006**, *6*, 845-857, DOI: 10.2174/138955706777934991.

[36] Lerín, C.; Montell, E.; Nolasco, T.; García-Rocha, M.; Guinovart, J. J.; Gómez-Foix, A. M., Regulation of glycogen metabolism in cultured human muscles by the glycogen phosphorylase inhibitor CP-91149, *Biochem. J.*, **2004**, *378*, 1073-1077, DOI: 10.1042/BJ20030971.

[37] Heightman, T. D.; Vasella, A.; Tsitsanou, K. E.; Zographos, S. E.; Skamnaki, V. T.; Oikonomakos, N. G., Cooperative Interactions of the Catalytic Nucleophile and the Catalytic Acid in the Inhibition of β-Glycosidases. Calculations and their validation by comparative kinetic and structural studies of the inhibition of glycogen phosphorylase b, *Helv. Chim. Acta*, **1998**, *81*, 853-864, DOI: org/10.1002/hlca.19980810507.

[38] Oikonomakos, N. G.; Skamnaki, V. T.; Ösz, E.; Szilágyi, L.; Somsák, L.; Docsa, T.; Tóth, B.; Gergely, P., Kinetic and Crystallographic Studies of Glucopyranosylidene Spirothiohydantoin Binding to Glycogen Phosphorylase b, *Biorg. Med. Chem.*, **2002**, *10*, 261-268, DOI: org/10.1016/S0968-0896(01)00277-2.

[39] Oikonomakos, N. G.; Kosmopoulou, M.; Zographos, S. E.; Leonidas, D. D.; Chrysina, E. D.; Somsák, L.; Nagy, V.; Praly, J.-P.; Docsa, T.; Tóth, B.; Gergely, P., Binding of N-acetyl-N′-β-d-glucopyranosyl urea and N-benzoyl-N′-β-d-glucopyranosyl urea to glycogen phosphorylase b, *Eur. J. Biochem.*, **2002**, *269*, 1684-1696, DOI: org/10.1046/j.1432-1327.2002.02813.x.

[40] Mitchell, E. P.; Withers, S. G.; Ermert, P.; Vasella, A. T.; Garman, E. F.; Oikonomakos, N. G.; Johnson, L. N., Ternary Complex Crystal Structures of Glycogen Phosphorylase with the Transition State Analogue Nojirimycin Tetrazole and Phosphate in the T and R States, *Biochemistry*, **1996**, *35*, 7341-7355, DOI: 10.1021/bi960072w.

[41] Oikonomakos, N. G.; Tiraidis, C.; Leonidas, D. D.; Zographos, S. E.; Kristiansen, M.; Jessen, C. U.; Nørskov-Lauritsen, L.; Agius, L., Iminosugars as Potential Inhibitors of Glycogenolysis: Structural Insights into the Molecular Basis of Glycogen Phosphorylase Inhibition, *J. Med. Chem.*, **2006**, *49*, 5687-5701, DOI: 10.1021/jm060496g.

[42] Oikonomakos, N. G.; Kontou, M.; Zographos, S. E.; Watson, K. A.; Johnson, L. N.; Bichard, C. J. F.; Fleet, G. W. J.; Acharya, K. R., N-acetyl-β-D-glucopyranosylamine: A potent T-state inhibitor of glycogen phosphorylase. A comparison with α-D-glucose, *Protein Sci.*, **1995**, *4*, 2469-2477, DOI: org/10.1002/pro.5560041203.

[43] Benltifa, M.; Hayes, J. M.; Vidal, S.; Gueyrard, D.; Goekjian, P. G.; Praly, J.-P.; Kizilis, G.; Tiraidis, C.; Alexacou, K.-M.; Chrysina, E. D.; Zographos, S. E.; Leonidas, D. D.; Archontis, G.; Oikonomakos, N. G., Glucose-based spiro-isoxazolines: A new family of potent glycogen phosphorylase inhibitors, *Biorg. Med. Chem.*, **2009**, *17*, 7368-7380, DOI: org/10.1016/j.bmc.2009.08.060.

[44] Chrysina, E. D.; Bokor, É.; Alexacou, K.-M.; Charavgi, M.-D.; Oikonomakos, G. N.; Zographos, S. E.; Leonidas, D. D.; Oikonomakos, N. G.; Somsák, L., Amide-1,2,3-triazole bioisosterism: the glycogen phosphorylase case, *Tetrahedron: Asymmetry*, **2009**, *20*, 733-740, DOI: org/10.1016/j.tetasy.2009.03.021.

[45] Manta, S.; Xipnitou, A.; Kiritsis, C.; Kantsadi, A. L.; Hayes, J. M.; Skamnaki, V. T.; Lamprakis, C.; Kontou, M.; Zoumpoulakis, P.; Zographos, S. E.; Leonidas, D. D.; Komiotis, D., 3′-Axial CH_2OH Substitution on Glucopyranose does not Increase Glycogen Phosphorylase Inhibitory Potency. QM/MM-PBSA Calculations Suggest Why, *Chem. Biol. Drug Des.*, **2012**, *79*, 663-673, DOI: org/10.1111/j.1747-0285.2012.01349.x.

[46] Forli, S.; Huey, R.; Pique, M. E.; Sanner, M. F.; Goodsell, D. S.; Olson, A. J., Computational protein-ligand docking and virtual drug screening with the AutoDock suite, *Nat. Protoc.*, **2016**, *11*, 905-919, DOI: 10.1038/nprot.2016.051.

[47] Gasteiger, J.; Marsili, M., A new model for calculating atomic charges in molecules, *Tetrahedron Lett.*, **1978**, *19*, 3181-3184, DOI: org/10.1016/S0040-4039(01)94977-9.

[48] Gasteiger, J.; Marsili, M., Iterative partial equalization of orbital electronegativity-a rapid access to atomic charges, *Tetrahedron*, **1980**, *36*, 3219-3228, DOI: org/10.1016/0040-4020(80)80168-2.

[49] Abraham, M. J.; Murtola, T.; Schulz, R.; Páll, S.; Smith, J. C.; Hess, B.; Lindahl, E., GROMACS: High performance molecular simulations through multi-level parallelism from laptops to supercomputers, *SoftwareX*, **2015**, *1-2*, 19-25, DOI: https://doi.org/10.1016/j.softx.2015.06.001.

[50] Bursulaya, B. D.; Totrov, M.; Abagyan, R.; Brooks, C. L., 3rd, Comparative study of several algorithms for flexible ligand docking, *J. Comput. Aided Mol. Des.*,

2003, *17*, 755-763, DOI: 10.1023/b:jcam.0000017496.76572.6f.

[51] Martin, J.; Veluraja, K.; Ross, K.; Johnson, L.; Fleet, G.; Ramsden, N.; Bruce, I.; Orchard, M.; Oikonomakos, N., Glucose analog inhibitors of glycogen phosphorylase: The design of potential drugs for diabetes, *Biochemistry*, **1991**, *30*, 10101-10116, DOI: 10.1021/bi00106a006.

[52] Wang, Z.; Sun, H.; Yao, X.; Li, D.; Xu, L.; Li, Y.; Tian, S.; Hou, T., Comprehensive evaluation of ten docking programs on a diverse set of protein–ligand complexes: the prediction accuracy of sampling power and scoring power, *Phys. Chem. Chem. Phys.*, **2016**, *18*, 12964-12975, DOI: org/10.1039/C6CP01555G.

[53] Cross, J. B.; Thompson, D. C.; Rai, B. K.; Baber, J. C.; Fan, K. Y.; Hu, Y.; Humblet, C., Comparison of several molecular docking programs: pose prediction and virtual screening accuracy, *J. Chem. Inf. Model.*, **2009**, *49*, 1455-1474, DOI: 10.1021/ci900056c.

[54] Kellenberger, E.; Rodrigo, J.; Muller, P.; Rognan, D., Comparative evaluation of eight docking tools for docking and virtual screening accuracy, *Proteins: Struct. Funct. Bioinform.*, **2004**, *57*, 225-242, DOI: 10.1002/prot.20149.

[55] Houston, D. R.; Walkinshaw, M. D., Consensus docking: improving the reliability of docking in a virtual screening context, *J. Chem. Inf. Model.*, **2013**, *53*, 384-390, DOI: org/10.1021/ci300399w.

[56] Tuccinardi, T.; Poli, G.; Romboli, V.; Giordano, A.; Martinelli, A., Extensive consensus docking evaluation for ligand pose prediction and virtual screening studies, *J. Chem. Inf. Model.*, **2014**, *54*, 2980-2986, DOI: org/10.1021/ci500424n.

[57] Prieto-Martínez, F. D.; Arciniega, M.; Medina-Franco, J. L., Molecular docking: current advances and challenges, *TIP Rev. espec. cienc. quím.-biol.*, **2018**, *21*, DOI: 10.22201/fesz.23958723e.2018.0.143.

[58] Salveson, P. J.; Haerianardakani, S.; Thuy-Boun, A.; Yoo, S.; Kreutzer, A. G.; Demeler, B.; Nowick, J. S., Repurposing triphenylmethane dyes to bind to trimers derived from Aβ, *J. Am. Chem. Soc.*, **2018**, *140*, 11745-11754, DOI: org/10.1021/jacs.8b06568.

[59] Corre, S.; Tardif, N.; Mouchet, N.; Leclair, H. M.; Boussemart, L.; Gautron, A.; Bachelot, L.; Perrot, A.; Soshilov, A.; Rogiers, A., Sustained activation of the Aryl hydrocarbon Receptor transcription factor promotes resistance to BRAF-inhibitors in melanoma, *Nat. Commun.*, **2018**, *9*, 1-13, DOI: org/10.1038/s41467-018-06951-2.

[60] Gaillard, T., Evaluation of AutoDock and AutoDock Vina on the CASF-2013 benchmark, *J. Chem. Inf. Model.*, **2018**, *58*, 1697-1706, DOI: 10.1021/acs.jcim.8b00312.

[61] Vu, V. V.; Hangasky, J. A.; Detomasi, T. C.; Henry, S. J.; Ngo, S. T.; Span, E. A.; Marletta, M. A., Substrate selectivity in starch polysaccharide monooxygenases, *J. Biol. Chem.*, **2019**, *294*, 12157-12166, DOI: org/10.1074/jbc.RA119.009509.

[62] Caffalette, C. A.; Corey, R. A.; Sansom, M. S.; Stansfeld, P. J.; Zimmer, J., A lipid gating mechanism for the channel-forming O antigen ABC transporter, *Nat. Commun.*, **2019**, *10*, 1-11, DOI: org/10.1038/s41467-019-08646-8.

[63] Grither, W. R.; Longmore, G. D., Inhibition of tumor–microenvironment interaction and tumor invasion by small-molecule allosteric inhibitor of DDR2 extracellular domain, *Proc. Natl. Acad. Sci. U. S. A.*, **2018**, *115*, E7786-E7794, DOI: 10.1073/pnas.1805020115.

[64] Noike, M.; Matsui, T.; Ooya, K.; Sasaki, I.; Ohtaki, S.; Hamano, Y.; Maruyama, C.; Ishikawa, J.; Satoh, Y.; Ito, H., A peptide ligase and the ribosome cooperate to synthesize the peptide pheganomycin, *Nat. Chem. Biol.*, **2015**, *11*, 71-76, DOI: org/10.1038/nchembio.1697.

[65] Nguyen, N. T.; Nguyen, T. H.; Pham, T. N. H.; Huy, N. T.; Bay, M. V.; Pham, M. Q.; Nam, P. C.; Vu, V. V.; Ngo, S. T., Autodock Vina Adopts More Accurate Binding Poses but Autodock4 Forms Better Binding Affinity, *J Chem Inf Model*, **2020**, *60*, 204-211, DOI: 10.1021/acs.jcim.9b00778.

[66] Cole, J.; Davis, E.; Jones, G.; Sage, C., *Molecular Docking-A Solved Problem?*, Reference Module in Chemistry, Molecular Sciences and Chemical Engineering, Elsevier: **2017**, pp. 297-318.